Case Studies in Chemical and Environmental Engineering 11 (2025) 101104

Contents lists available at ScienceDirect

Case Studies in Chemical and Environmental Engineering

journal homepage: www.sciencedirect.com/journal/case-studies-in-chemical-and-environmental-engineering

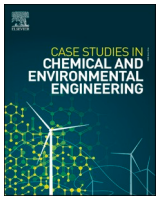

Case Report

Evaluation and comparison of drying models in open sun drying and photovoltaic and LPG burner assisted hybrid solar drying system

Tubagus Rayyan Fitra Sinuhaji, Suherman Suherman *, Hadiyanto Hadiyanto, Ardi Ardan, Sulistia Rahmawati

Department of Chemical Engineering, Faculty of Engineering, Diponegoro University, 50275, Semarang, Indonesia

ARTICLE INFO

Keywords:
Dried cacao beans
Drying kinetics
Evaluation & comparison drying cacao
Open sun drying
And photovoltaic and LPG burner assisted hybrid solar drying system

ABSTRACT

This study evaluates the drying performance of open sun drying (OSD) and photovoltaic and LPG burner assisted hybrid solar drying system (HSD) systems for cocoa beans. OSD, a traditional and cost-effective method, faces limitations such as extended drying times, susceptibility to environmental contamination, and inconsistent quality. In contrast, HSD integrates solar energy with auxiliary heat sources, providing controlled drying conditions and improved efficiency. The research involved experimental comparisons between the two methods, using cocoa beans as the primary material. Measurements included temperature, relative humidity, drying duration, and energy utilization. Data were analyzed with thin-layer drying models, with the Midili model being the most accurate ($R^2 > 0.98$). Drying trials were conducted at 40 °C, 45 °C, and 50 °C, with the target moisture content set at 7–8%. Results showed that HSD achieved superior performance, reducing drying times to 3–4 hours compared to 23 hours for OSD. HSD also demonstrated higher exergy efficiencies (94.6614 %) and lower exergy loss (0.0062 kJ/s). Furthermore, the controlled environment minimized contamination risks and preserved the quality of the cocoa beans. This study concludes that HSD significantly enhances drying efficiency, product quality, and sustainability compared to OSD. These findings suggest that hybrid drying technologies hold great potential for modernizing agricultural drying practices while addressing energy and environmental challenges.

1. Introduction

Open sun drying (OSD) of cacao is a traditional method that uses natural solar energy to reduce the moisture content in cocoa beans. This method is widely practiced because it is simple and cost-effective; however, it also presents challenges concerning quality control and environmental factors. OSD utilizes direct solar radiation, spreading beans on surfaces like cement yards or wooden structures. The drying process is influenced by the intensity of the sun, the ambient temperature, and the humidity, which can lead to variable drying times, which can often take up to 3.5 days during the dry season [1]. Effective diffusivity values for OSD have been reported to be approximately 4.25×10^{-11} m^2/s, which indicates the rate at which moisture is removed from the beans [2]. Drying in the open sun can lead to contamination by dust, fungi, and pests, which can affect the safety and market value of the beans [1]. Quality parameters such as moisture content, color, and acidity are critical, and studies show that drying conditions have a significant impact on these factors [3]. While OSD is widely used, alternative methods such as solar dryers with thermal storage systems can improve drying efficiency and quality by providing controlled conditions. These systems can maintain optimal temperatures even during periods of low sunlight, reducing the risk of contamination and improving overall product quality [4].

Hybrid solar drying (HSD) for cocoa beans combines solar energy with other heat sources to improve drying efficiency and quality. This method has shown promising results in various studies, demonstrating significant improvements in moisture content and drying time compared to traditional methods. OSD and HSD represent two approaches to dehydrating agricultural products, each with unique advantages and limitations. OSD relies solely on solar energy, making it a low-cost method but vulnerable to environmental factors such as rain and pests. On the other hand, HSD integrates additional energy sources to improve efficiency and product quality. The following sections describe the key aspects of both methods. Hybrid solar dryers significantly reduce drying time compared to OSD. For example, red chili dried in a biogas

* Corresponding author.
E-mail addresses: eaglefansrayyan@gmail.com (T.R.F. Sinuhaji), suherman.mz@undip.ac.id (S. Suherman).

https://doi.org/10.1016/j.cscee.2025.101104
Received 2 December 2024; Received in revised form 23 December 2024; Accepted 9 January 2025
Available online 19 January 2025

Nomenclature

A	Area (m^2)
A	Coefficient
a, b, c	Coefficient in kinetics modeling
Cp	Specific heat capacity (kJ/K.°C)
D_{eff}	Effective moisture diffusivity
DR	Drying rate ($hour^{-1}$)
EU	Energy utilization (kJ/s)
EUR	Energy utilization ratio
EX	Exergy rate (kJ/s)
h	Entalphy (kJ/kg)
h_{fg}	Latent heat of vaporization (kJ/kg)
HSD	Hybrid solar drying or Photovoltaic and LPG burner assisted hybrid solar drying system
IP	Improvement potential rate (kJ/s)
LPG	Liquified Petroleum Gas
k	Drying constant
MC	Moisture content
MR	Moisture ratio
N	Total data
OSD	Open sun drying
P	Pressure (Pa)
PV	Photovoltaic
Q	Heat transfer (kJ/s)
R	specific function of independent variables
R^2	Correlation coefficient
RMSE	Root mean square error
SI	Sustainability index
T	Temperature (°C)
t	Time (hour)
V	Air velocity (m/s)
w_R	Uncertainties of the independent variable

Greek Symbol

ρ	Density(kg/m^3)
φ	Relative humidity of air (%)
χ^2	Chi-square
ω	Humidity ratio (kg water/kg dry air)

Subscripts

0	Initial
∞	Ambient
a	Air
da	Dried air
dc	Drying chamber
dp	Dried product
e	Equilibrium
evp	Evaporation
fp	Fresh product
hdb	Hybrid dryer body
ij	Numerator
in	Inlet
L	Heat loss
out	Output or Outlet
p	Pressure
ph	Physical
tp	Triple point
vs	Saturated vapor
w.b	Wet basis

hybrid mode took 14 hours, while OSD took 28 hours to reach similar moisture levels [5]. A hybrid solar dryer for cassava achieved a moisture reduction from 65 % to 10.19 % in 7 hours compared to 35 hours for OSD [6]. A prototype mixed solar dryer achieved a final moisture content of 10.31 % with an efficiency of 22.82 % and a specific energy consumption of 2.75 kWh/kg [7].

HSD and OSD of cocoa beans present different advantages and challenges in drying. Studies indicate that hybrid solar dryers can achieve moisture content as low as 10.31 % with a drying rate that is double that of OSD, which typically results in higher final moisture content (17.4 %) [7,8]. OSD is highly dependent on weather conditions, resulting in inconsistent drying rates and potential contamination from environmental factors [9]. HSD not only reduces drying time but also minimizes the risk of mold and preserves the quality of the cocoa beans, as evidenced by lower fat content and better overall quality parameters [3]. Exposure to UV radiation and environmental contaminants can adversely affect the quality of cocoa beans dried in the open air (OSD) [9]. HSD has a specific energy consumption of 2.75 kWh/kg, demonstrating their efficiency in energy use compared to traditional methods [7]. While HSD offers significant efficiency and quality preservation advantages, OSD remains a widely used method due to its simplicity and low cost. However, the potential for improved quality of the exergy efficiency of systems can vary, with reported values ranging from 22.77 % to 27.90 %, indicating significant potential for energy utilization processing.

Photovoltaic and LPG burner assisted hybrid solar drying systems integrate photovoltaic (PV) technology with thermal energy sources to improve drying efficiency and sustainability. These systems use solar energy to power the drying process while incorporating additional heating methods, such as burners or heat pumps, to maintain optimal drying conditions, especially in low sunlight or high-humidity environments. Hybrid systems exhibit high energy efficiencies, with reported thermal efficiencies of up to 72.36 % and overall efficiencies of around 47.7 % [10,11]. The exergy efficiency of systems can vary, with reported values ranging from 22.77 % to 27.90 %, indicating significant potential for energy utilization [12]. The integration of PV systems in drying processes can lead to significant CO_2 reductions, with one study reporting a net reduction of 60.29 tons of CO_2 [10]. These systems promote environmental benefits by reducing dependence on fossil fuels and increasing the use of renewable energy sources [12]. Payback periods for these systems are favorable, with some studies showing periods as short as 1.5–2.7 years, making them economically attractive for agricultural applications [10,13].

The evaluation of drying models for cocoa beans includes various methods and technologies to optimize the drying process. Research shows that different drying techniques and conditions have a significant impact on the moisture content and quality of cocoa beans. Studies have shown that the drying kinetics of cacao beans, particularly Criollo and Forastero varieties, can be effectively modeled using the Midili model, which demonstrated high accuracy ($R^2 > 0.998$) across various temperatures (50 °C, 60 °C, 70 °C). The drying rate increases with temperature, with 60 °C yielding optimal moisture content (8.15 % for Criollo and 8.89 % for Forastero) [14]. Thus, the current study is to evaluate the drying process with various drying models between open drying and drying using a photovoltaic and LPG burner assisted hybrid solar drying system.

2. Materials and methods

2.1. Materials

The materials used in the study were cocoa beans obtained from Kudus Regency, Central Java Province, Indonesia (6°43′15.3″ S 110°52′36.7″ E).

2.2. Measuring tools and experimental set-up

This research was conducted at the Chemical Engineering Waste Treatment Laboratory, Diponegoro University. The experimental setup is shown in Fig. 1. Various measuring instruments are used to ensure that the cocoa beans are properly dried during the drying process. A digital kitchen scale was used to measure the weight of the cocoa bean samples. Sunlight intensity was measured using a UNI-T UT383 mini light meter, while air speed was measured using an ANENG GN301 digital anemometer. To measure the ambient temperature and relative humidity of the environment, the Smart Sensor AS847 humidity and temperature meter was used. To ensure accurate temperature measurements in the drying chamber, thermocouples were installed on each tray. Further specifications regarding the instruments in this study are presented in Table 1.

The model of the photovoltaic and LPG burner assisted hybrid solar drying system is illustrated in Fig. 2. The drying system comprises two main components: a drying chamber and solar collectors. The drying chamber measures 1.00 m × 0.60 m × 0.94 m, and cocoa beans are placed on a tray that has dimensions of 0.56 m × 0.45 m. The solar collector is a flat plate type, with a size of 1 m^3. It features a black-painted absorber made of 1 mm PVC and a glass cover that is 2 mm thick. The solar collector is oriented toward the north with a tilt angle of 40° [15]. In addition, the blower that channels hot air from the solar collector to the drying chamber is powered by energy generated from solar photovoltaic panels with MY50M − 12 specifications. These PV modules are made from polycrystalline silicon solar cells and have dimensions of 0.6 m × 0.5 m. The system includes a battery with a capacity of 14V/80 Ah and a DC fan rated at 12V/0.14 A. This research is designed to operate using electricity supplied from the battery connected to the PV module, as discussed in the study by Afzal et al. [16].

2.3. Experimental procedure

The incoming cocoa is cleaned by washing and soaking to remove the dirt from the cocoa skin. Before being dried, the freshly harvested cocoa beans are fermented for five days in Styrofoam boxes. The specific fermentation methods are documented elsewhere [17]. The method is measured by the furnace and calculated from the mass lost at a temperature of 105–110 °C to obtain a constant weight [18]. This research was conducted for about 8 hours of effective time (8 a.m.–4 p.m.) with 2 drying methods, using OSD and HSD, temperature control was carried out by adjusting the system in the burner when the temperature was reached, and the temperature range was 40, 45, 50 °C [13].

Fig. 1. Experimental setup of photovoltaic and LPG burner assisted hybrid solar drying system.

Table 1
Specifications of the instruments used.

No.	Device	Model and uses	Range	Accuracy
1.	Digital anemometer	ANENG GN-301 and measure the air velocity	0.4–30 m/s	± (3 % + 0.3 m/s)
2.	Digital kitchen scale	JOIL and measure the mass of the product	3–500 g	±0.01 g
3.	Humidity & temperature meter	Smart Sensor AS847 and measure the humidity and temperature	5.0–98 % RH 0.0–100 °C	±3.5 % RH ±0.01 °C
4.	Mini light meter	UNI-T UT383 and measure the solar intensity	0–9999 lux ≥10,000 Lux	± (4 % rdg + 8 dgts) ± (5 % rdg +10 dgts)
5.	Thermocouple	Stainless steel and measure a temperature in the chamber	0.0–100 °C	±0.5 °C

Take place a 300-g sample on each tray of the solar dryer. Temperature, RH, solar intensity, and cocoa bean mass were measured hourly with the appropriate equipment. The air temperatures of the inlet, drying chamber, and outlet of the dryer were also measured. At the end of the effective drying time, the sample is sealed in an airtight plastic container at room temperature and the process is continued the next day. The drying process was stopped when the moisture content of the cocoa beans fell below 7–8% [19–23].

2.4. Data analysis

2.4.1. Temperature profile

For drying hours, take an hourly temperature reading on each tray, taking note of the temperature at the inlet, outlet, outside air, and drying chamber of the solar dryer. Make a judgment based on the temperature data and operation time. To illustrate how the temperature fluctuates over time, plot a graph [24].

2.4.2. Drying curve analysis

2.4.2.1. Moisture content. To determine the moisture content, we must weigh the sample on each tray every hour and plot the moisture content against time. The equation is as follows [15,24]:

$$MC = \frac{m_i - m_d}{m_i} x\ 100 \quad (1)$$

Where M_i is initial mass (g); M_d is mass after drying (g); MC is moisture content.

2.4.2.2. Moisture ratio. The moisture content data obtained from the experimental data were converted to moisture ratio (MR) using the equation [25]:

$$MR = \frac{M - M_e}{M_i - M_e} = Ae^{-kt} \quad (2)$$

Where MR is the moisture ratio, M_i is the initial moisture content, M_e is the equilibrium moisture content (±7.00 %), M is the moisture content at any time, k is the drying constant (d^{-1}), t is the time (d), and A is a coefficient.

2.4.2.3. Dehydration ratio. The weight of the samples was measured, then dried and weighed again. The dehydration ratio was calculated from the resulting weight difference and given as an equation [26]:

$$\text{Dehidration Ratio} = \frac{\text{Weight of prepared material}}{\text{Weight of dried material}} \quad (3)$$

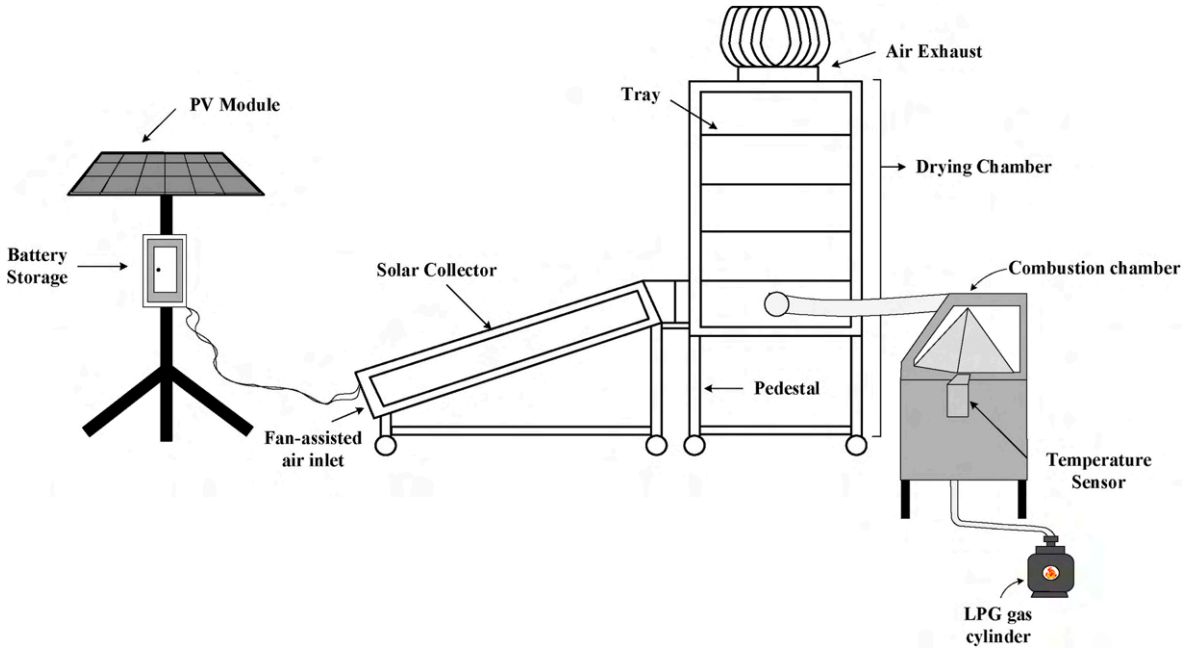

Fig. 2. Illustration of a photovoltaic and LPG burner assisted hybrid solar drying system.

2.4.2.4. Drying rate. The drying rate equation is critical in understanding moisture loss kinetics during drying processes. The drying rate is described in the following equation [27]:

$$DR = \frac{M_t - M_{t+\Delta t}}{\Delta t} \quad (4)$$

Where DR is the drying rate, M_t is the moisture content in t time, and $M_{t+\Delta t}$ is the moisture content after t time.

2.4.3. Thin layer drying

Thin layer approach models, which are referred to as semi-theoretical and empirical models, were employed. Three parameters were used to evaluate the accuracy of the drying models - the correlation coefficient (R^2), the root mean square error (RMSE), and the chi-square (χ^2). The best model is selected based on the highest value of R^2 and the lowest value of RMSE and chi-square (χ^2). We can determine the value of R^2, χ^2, and RMSE using the following equation [15,28]:

$$RMSE = \sqrt{\frac{1}{N}\sum_{i=1}^{N}\left(MR_{exp,i} - MR_{pre,i}\right)^2} \quad (5)$$

$$R^2 = \frac{\left[\sum_{i=1}^{N}\left(MR_{exp,i} - \overline{MR_{exp}}\right)\left(MR_{pre,i} - \overline{MR_{pre}}\right)\right]^2}{\sum_{i=1}^{N}\left(MR_{exp,i} - \overline{MR_{exp}}\right)^2 \sum_{i=1}^{N}\left(MR_{pre,i} - \overline{MR_{pre}}\right)^2} \quad (6)$$

$$\chi^2 = \frac{\left[\sum_{i=1}^{N}\left(MR_{exp,i} - \overline{MR_{exp}}\right)\left(MR_{pre,i} - \overline{MR_{pre}}\right)\right]^2}{N - z} \quad (7)$$

It is important to note that some semi-theoretical models only consider the external resistance to moisture transport at the feedstock-air interface. These models are based on Newton's law of cooling or a modified version of Fick's II law of diffusion. They are effective even though they are straightforward and just call for a few presumptions. Furthermore, several researchers have created several semi-theoretical drying models for a range of situations. Empirical models rely on experimental settings, have no physical explanation, and solely consider external barriers to moisture transport. An alternative is to use empirical drying models [29].

The nine thin-layer models were fitted to analyze the experimental results of MR for cacao beans, using statistical tools such as correlation coefficient (R^2), Root Mean Square Error (RMSE), and chi-square (χ^2). Below are the nine used in this drying model and tabulated in Table 2.

2.4.4. Energy and exergy analysis

2.4.4.1. Energy utilization (EU) [27]. To do an energy analysis using equations (17)–(20), the drying process of the cocoa beans was regarded as a stable flow process. Equation (19), a general energy conversion equation, was used to examine the energy balance of the dryer's input and output flows. The air properties, such as the dry air density and the dry air enthalpy, were determined using equations (17) and (18). Furthermore, the energy utilization (EU) was computed using Equation (19):

$$\rho_a = \frac{101.325}{0.287\ (T_a + 273.16)} \quad (17)$$

Table 2
Nine models were used in this study.

Model	Equation
Newton/Lewis (semi-theoretical – Newton's law of cooling) [30]	$MR = \exp(-kt)$ (8)
Page (semi-theoretical – Newton's law of cooling) [30]	$MR = \exp(-kt^n)$ (9)
Handerson-Pabis (semi-theoretical – Fick's II law of diffusion) [30]	$MR = a\exp(-kt)$ (10)
Two-term (semi-theoretical – Fick's II law of diffusion) [30]	$MR = a\exp(-k_1 t) + b\exp(-k_2 t)$ (11)
Logarithmic (semi-theoretical – Fick's II law of diffusion) [31]	$MR = a\exp(-kt) + C$ (12)
Midilli (semi-theoretical – Fick's II law of diffusion) [32]	$MR = a\exp(-kt^n) + bt$ (13)
Weibull (empirical) [29,33]	$MR = \exp\left[-\left(\frac{t}{\alpha}\right)^{\beta}\right]$ (14)
Wang & Singh (empirical) [29]	$MR = 1 + bt + at^2$ (15)
Aghbashlo (empirical) [29]	$MR = \exp(-k_1 t/(1+k_2 t))$ (16)

$$h_a = c_a(T_a - T_\infty) + h_{fg}\omega \tag{18}$$

$$EU = \dot{m}_{ina}h_{ina} + \dot{m}_{fp}h_{fp} - \dot{m}_{outa}h_{outa} - \dot{m}_{dp}h_{dp} - \dot{Q}_L \tag{19}$$

$$\dot{Q}_{evp} = \dot{m}_{ina}h_{fg}\omega \tag{20}$$

2.4.4.2. Energy utilization ratio (EUR) [27]. Equation (21) was used to determine the specific heat of the input or output product before calculating the enthalpy of the fresh and dry goods. The specific heat capacity of the dryer's input and exit air was also calculated using equation (22). Equation (23) was used to determine the humidity rate. Lastly, the energy utilization ratio (EUR) and the rate of heat loss from the dryer body and the air exiting the dryer were computed using equations (24)–(27).

$$h_b = c_p(T_b - T_\infty) \tag{21}$$

$$c_{pa} = 1.004 + 1.88\omega \tag{22}$$

$$\omega = 0.622\frac{\varphi P_{vs,a}}{P - \varphi P_{vs,a}} \tag{23}$$

$$\dot{Q}_{al} = \dot{m}_{ina}c_{pda}(T_{ina} - T_{ina}) \tag{24}$$

$$\dot{Q}_{hdb} = UA_{hdb}(T_{tp} - T_\infty) \tag{25}$$

$$U = \frac{\dot{m}_{ina}c_{pina}(T_{ina} - T_{outa})}{A_{hdb}(T_{tp} - T_\infty)} \tag{26}$$

$$EUR = \frac{\dot{m}_{ina}h_{ina} + \dot{m}_{fp}h_{fp} - \dot{m}_{outa}h_{outa} - \dot{m}_{dp}h_{dp} - \dot{Q}_L}{\dot{m}_{ina}(h_{ina} - h_\infty)} \tag{27}$$

2.4.4.3. Exergy evaluation [27]. The first and second laws of thermodynamics were generally followed when performing the exergy analysis. Equation (28) through (30) were used to determine the dryer chamber's specific exergy of air, exergy loss, and exergetic efficiency. The greatest increase in energy efficiency is attained when a system's irreversibility or energy loss is minimal. Equation (31) was utilized to determine the rate of exergy improvement potential. Lastly, equation (32) was used to calculate the drying process's sustainability index (SI).

$$ex_{da} = c_{pda}(T - T_0) - T_0\left[c_{pda}\ln\frac{T}{T_0}\right] + T_0\left[R\ln\frac{(1 + 1.6078\omega_0)}{(1 + 1.6078\omega)}\right] + 1.6078\omega R\ln\left(\frac{\omega}{\omega_0}\right) \tag{28}$$

$$Ex_L = Ex_{in} - Ex_{out} \tag{29}$$

$$\varphi_{ex} = \frac{Ex_{in} - Ex_L}{Ex_{in}} \tag{30}$$

$$IP = (1 - \varphi_{ex})(Ex_{in} - Ex_{out}) \tag{31}$$

$$SI = \frac{1}{1 - \varphi_{ex}} \tag{32}$$

2.4.5. Uncertainty analysis

Uncertainty analysis is a useful method when analyzing experimental data. Human error, instrument selection, calibration, experimental settings, and observations can all lead to uncertainty. The uncertainty in the outcome linked to that probability, assuming that the uncertainties in the independent variables are equally likely as follows [19]:

$$R = R(x_1, x_2, x_3, \ldots x_n) \tag{33}$$

$$w_R = \left[\left(\frac{\partial R}{\partial x_1}w_1\right)^2 + \left(\frac{\partial R}{\partial x_2}w_2\right)^2 + \ldots + \left(\frac{\partial R}{\partial x_3}w_3\right)^2\right]^{\frac{1}{2}} \tag{34}$$

The experiment estimates and describes the uncertainties of both the independent and dependent variables; these are listed in Table 3.

3. Results and discussion

3.1. Temperature profile and weather conditions in the drying process

The temperature profile during the drying process is crucial for determining the efficiency and quality of the final product. Numerous studies have examined how temperature influences drying kinetics, moisture content, and product characteristics [34–36]. Environmental conditions, such as temperature, relative humidity, and airflow, greatly affect drying. Understanding these factors is essential for enhancing drying efficiency for agricultural products like grains. Figs. 3–6 shows the three-variable relationship between relative humidity, temperature, and intensity on OSD and HSD.

Fig. 3 shows the data of the OSD process for several days (Day 1, Day 2, and Day 3) and the combined data for a total of 23 hours of drying. The variables analyzed were Temperature (°C), Sunlight Intensity (W/m^2), and Relative Humidity (%) against time. In Fig. 3a, temperature, sunlight intensity, and humidity show a related pattern—sunlight intensity peaks between 11:00 and 13:00, coinciding with the maximum temperature. Humidity decreases drastically during the daytime period. Fig. 3b shows a similar pattern, with peak sunlight intensity around 12:00–14:00. Temperature increases with sunlight intensity, while relative humidity decreases during the day. In Fig. 3c, data is only available until midday because the drying time has been completed until the target moisture content has been achieved. The pattern of increasing temperature and sunlight intensity is seen until 11:00, then tends to be stable. Humidity decreases sharply during the morning period. Fig. 3c shows the trend during 23 hours of drying time. Temperature and sunlight intensity peaked at noon, while relative humidity reached its minimum value during the same period.

In weather conditions such as tropical climates with high humidity, high relative humidity can interfere with the drying process [37]. Seasonal temperature changes affect drying times; for example, summer conditions allow for faster drying compared to the winter or the rainy season in tropical countries [38]. The effect of the temperature profile is to significantly reduce drying time and maintain nutritional quality with optimal drying temperatures of 48 °C–68 °C [39]. However, temperature variations within the drying bed can lead to quality issues, such as cracks in cocoa beans, which affect the cacao yields [40].

Fig. 4 shows data on the HSD process at 40 °C for several days (Day 1, Day 2, and Day 3) and a combined graph for the drying process using the hybrid system. This data involves the same three main parameters as OSD, namely: Temperature (°C), Sunlight Intensity (W/m^2), and

Table 3
Estimated value for the uncertainty in the experiment.

Parameter	Uncertainty value
Air velocity in the collector	±0.0890 m/s
Air velocity in the chamber	±0.0455 m/s
Ambient air temperature	±0.16 °C
Ambient relative humidity	±0.52 %
Drying rate	±1.4730 g. water/g. dry matter. hour
Energy utilization	±8.5239 kJ/s
Energy utilization ratio	±0.0531
Exergy efficiency	±0.0558 %
Exergy loss rate	±0.0107 kJ/s
Improvement potential rate	±0.0040 kJ/s
Mass of product	±2.4611 g
Moisture content	±1.93 %
Sustainability index	±3.3595

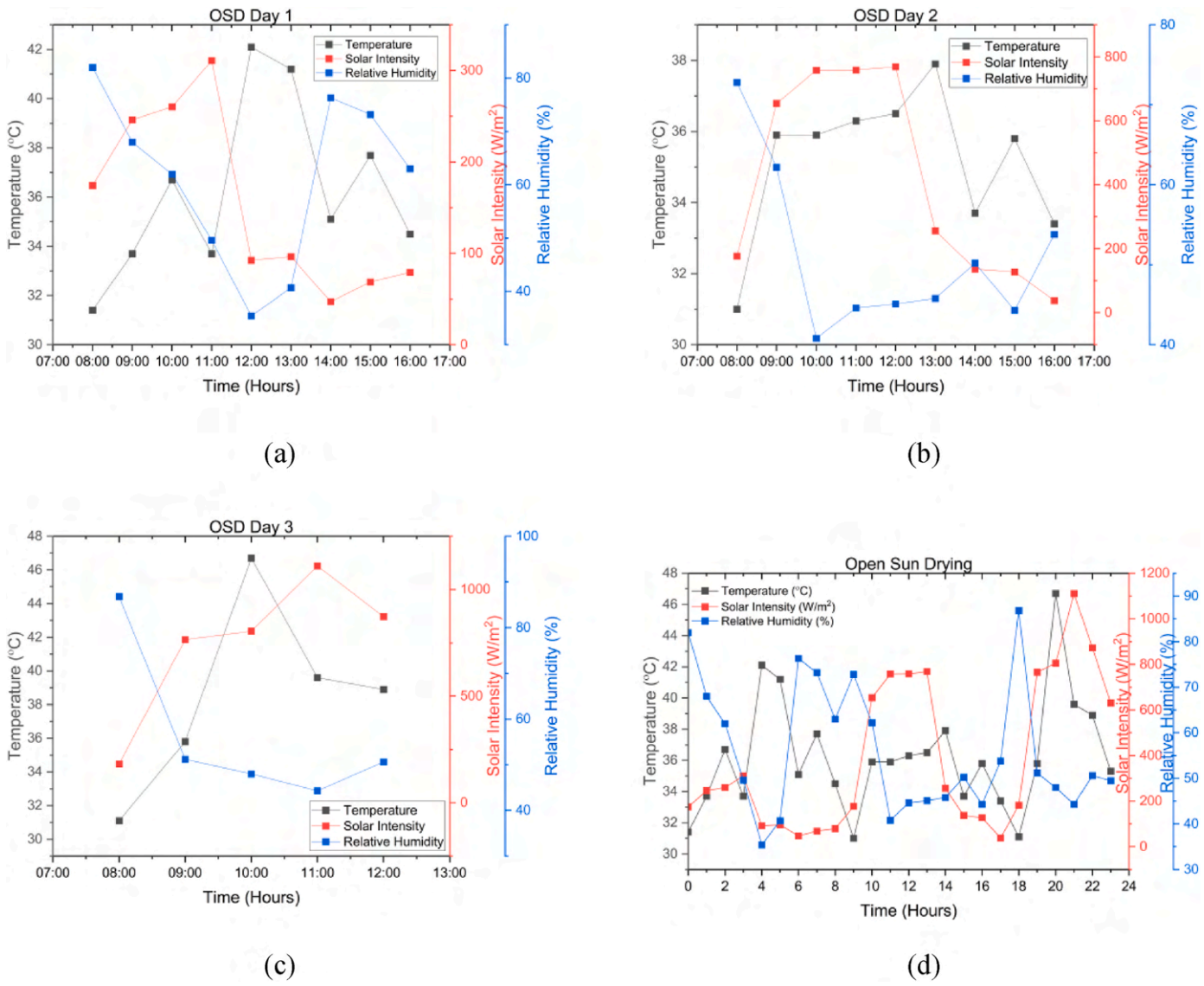

Fig. 3. Temperature profile and weather conditions on OSD; (a) day 1; (b) day 2; (c) day 3; and (d) overall.

Relative Humidity (%) against time. Fig. 4a shows drying on day 1, temperature and sunlight intensity increased gradually from morning to noon, with a peak around 12:00–14:00. Relative humidity decreased during the day, supporting the drying process because the air became drier. Fig. 4b shows a similar pattern to day 1, but the temperature and sunlight intensity fluctuations appear more regular. The decrease in relative humidity co-occurs with the increase in temperature, indicating ideal conditions for drying. Fig. 4c shows drying until 13:00, which is similar to Days 1 and 2. Relative humidity decreased sharply from the morning to noon, supporting the drying process. Fig. 4d shows the fluctuations over a full 20 hours for the hybrid system. The temperature remained controlled at around 40 °C throughout the day, indicating that the hybrid system was able to maintain consistent drying conditions. The sunlight intensity peaked during the day, while the relative humidity was low during that period.

Fig. 5 shows the HSD process at 45 °C for several days (Day 1, Day 2, and Day 3), and the combined graph for the entire process is the same as before. In Fig. 5a, the temperature varies close to 45 °C throughout the day, indicating effective temperature control by the hybrid system. The sunlight intensity increases to a peak during the day (around 12:00–14:00). The relative humidity decreases drastically during the day, which supports the drying efficiency. Fig. 5b shows the fluctuation patterns of temperature, sunlight intensity, and relative humidity similar to those in Fig. 5a. The temperature remains stable at around 45 °C, indicating that the hybrid system can maintain the target temperature despite varying sunlight intensity. Relative humidity shows a decrease during the day, inversely proportional to the increase in temperature. Fig. 5c shows that drying ended at 10:00. The temperature tends to be close to stable, but the sunlight intensity has not reached its peak in the morning period. Relative humidity is still high due to the low sunlight intensity. Fig. 5d is a combined graph showing the parameter fluctuations during the drying process using the hybrid system. The temperature was maintained at around 45 °C throughout, although the sunlight intensity and relative humidity experienced large fluctuations. The hybrid system was proven to reduce the influence of environmental variables, creating more consistent drying conditions and a total drying stage achieved in 17 hours.

Fig. 6 shows the HSD process data at 50 °C, covering several days. However, only Day 1 and Day 2 because drying was completed faster compared to 40 °C and 45 °C, and the combined graph over the drying period. Fig. 6a shows that the temperature remains controlled and can be identified around 50 °C throughout the day despite the fluctuations in sunlight intensity and relative humidity. The sunlight intensity peaks at noon (around 12:00–14:00), which is accompanied by a decrease in

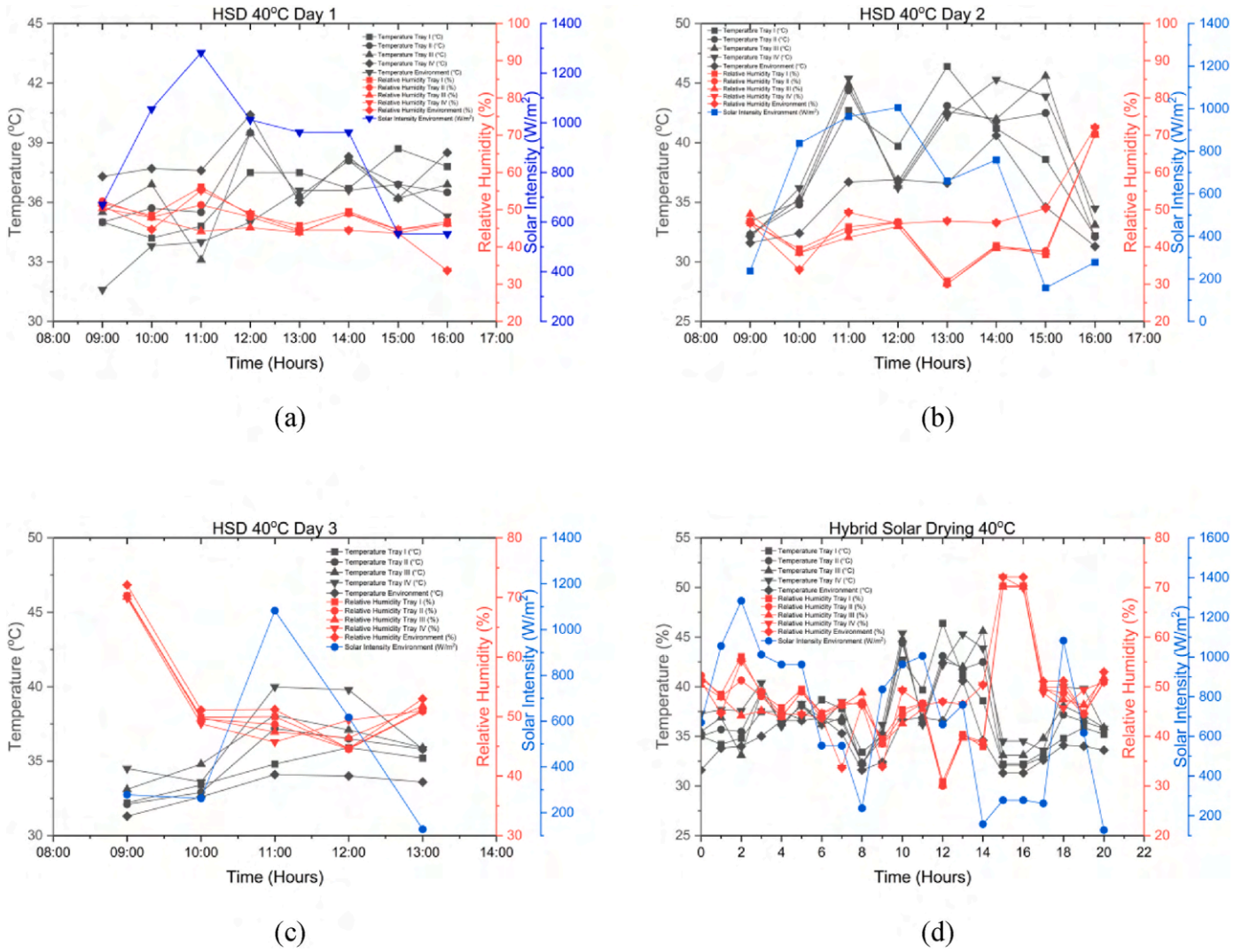

Fig. 4. Temperature profile and weather conditions on HSD 40 °C; (a) day 1; (b) day 2; (c) day 3; and (d) overall.

relative humidity. The decrease in relative humidity also helps accelerate the drying process, indicating that the hybrid system works effectively. Fig. 6b also shows a stable temperature of around 50 °C, despite the same variation in sunlight intensity as before. In the morning to afternoon period, the sunlight intensity increases sharply, accompanied by a decrease in relative humidity. This graph shows that the hybrid dryer system can maintain the optimal temperature, despite changes in environmental conditions. Fig. 6c is a combined graph showing the parameter fluctuations during drying at 50 °C. The temperature remained consistent at 50 °C, although the sunlight intensity showed significant fluctuations. Similarly, the relative humidity tended to be low during the day, indicating a very ideal environment for fast drying with a drying duration of 50 °C of 13 hours. Farmers and cocoa processors are encouraged to adopt HSD systems to reduce drying times significantly while achieving consistent product quality, HSD offers a reliable alternative to OSD.

Hybrid solar dryers are designed to optimize temperature control through solar energy and additional heating mechanisms. This dual approach makes it possible to maintain consistent and adjustable temperature profiles, which can be a critical factor in effective drying. For example, temperatures can be maintained at values between 40 °C and 50 °C, depending on the specific requirements of the dried material. The temperature inside a hybrid solar dryer will fluctuate with the intensity of the solar radiation throughout the day. Typically, when the sun's rays are most intense, the highest temperatures occur at midday. The higher temperatures in the hybrid dryer also contribute to a lower relative humidity level in the drying chamber. As the temperature of the air increases, its ability to hold moisture increases, resulting in a more effective evaporation of moisture from the product being dried. This is particularly beneficial as lower relative humidity ensures efficient drying [41–43].

3.2. *The effect of drying temperatures on drying kinetics*

Higher drying temperatures generally resulted in higher drying rates. Higher temperatures correspond to faster drying and shorter drying times [44,45]. The effective moisture diffusivity (D_{eff}) increases with higher temperatures warmer air enhances moisture movement from within the material to its surface [46,47]. A higher temperature increases the drying rate and reduces the total drying time. As seen in the comparison between temperatures (40 °C, 45 °C, 50 °C), temperature 50 °C greatly reduces the drying time [46]. The relationship between moisture content and temperature is complex; as moisture is removed, the drying rate typically decreases due to reduced moisture availability at the surface. However, maintaining higher temperatures can counteract this slowdown by increasing evaporation rates. The temperature of agricultural products in solar dryers is influenced by solar radiation and ambient conditions, affecting moisture content and product quality

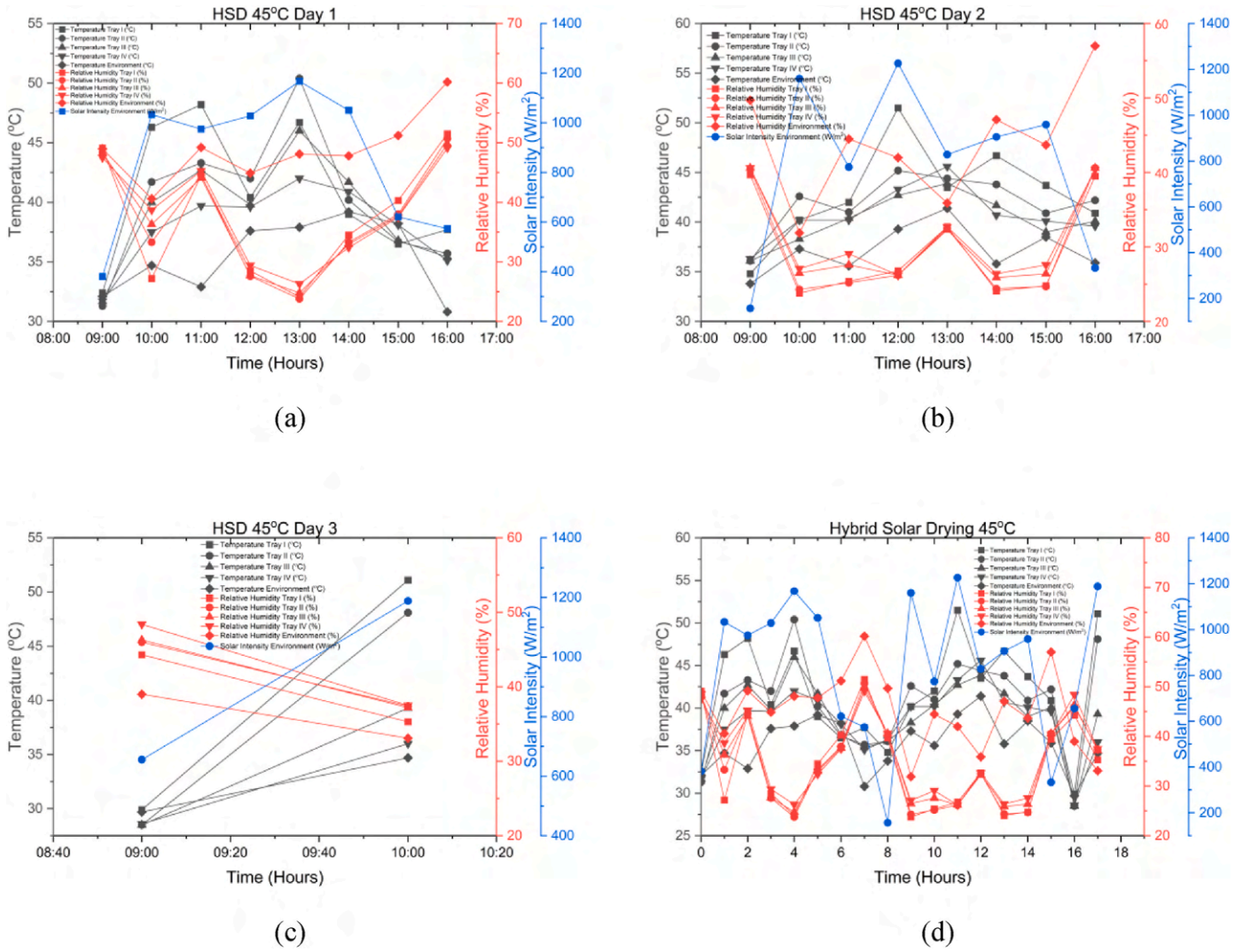

Fig. 5. Temperature profile and weather conditions on HSD 45 °C; (a) day 1; (b) day 2; (c) day 3; and (d) overall.

[48]. Fig. 7 shows the effect of changes in moisture content, moisture ratio, and dehydration ratio on drying time.

Fig. 7 shows that the HSD method with higher temperatures (45 °C and 50 °C) is more efficient than OSD. HSD temperature of 45 °C gives the best balance for drying speed. Compared to HSD, OSD takes longer because it is affected by fluctuations in temperature and humidity of the environment. The moisture ratio during the drying process is determined by the moisture content at any given time relative to the initial moisture content [49]. HSD at higher temperatures (50 °C) produces the fastest and most efficient dehydration. HSD at 45 °C provides a good alternative for materials that require protection from extreme temperatures but still want a high drying rate. Compared to HSD, OSD requires a longer time to achieve the same level of dehydration. Different materials exhibit unique moisture transfer behaviors. For instance, tomatoes showed an optimum moisture ratio of 0.774 under specific conditions [50]. The inherent properties of the dried material (e.g., porosity, size, and composition) also influence its moisture transfer behavior and thus its dehydration ratio. Smaller particle sizes typically result in higher dehydration ratios due to the increased surface area available for moisture removal [26]. Superior water vapor permeability can emphasize the importance of raw material properties over thickness [51]. Moisture must first cross cell membranes before it can move through extracellular spaces. This two-step process is critical in plant materials where moisture is primarily intracellular. Plant materials are often modeled as porous media, with moisture trapped in a network of cells and intercellular spaces. This model helps to simulate drying processes effectively [52,53].

In general, the drying rate is increased by increasing the air temperature. Higher temperatures increase the moisture-carrying capacity of the air. This allows the air to absorb more moisture from the material being dried. The drying time was significantly reduced at higher temperatures compared to lower temperatures due to the increased rate of evaporation [54]. Fig. 8 shows the relationship between drying time and drying rate, temperature, and moisture content. Furthermore, it explains the 3D relationship profile between drying rate-temperature-moisture content. The initial drying rate (0–4 h) was high for all temperatures, especially at 50 °C, indicating significant initial moisture removal. After a certain time, the drying rate decreased gradually as the moisture content of the material decreased, resulting in a slower evaporation process. HSD at 50 °C showed the highest drying rate consistently, while HSD at 40 °C had the lowest drying rate. The temperatures for each HSD method remained stable around their respective targets: 40 °C, 45 °C, and 50 °C. Higher temperatures (50 °C) favored faster drying rates because they increased the capacity of the air to hold moisture. The moisture content decreased significantly at the beginning of drying (0–6 h), especially at 50 °C, indicating higher drying efficiency. After 12 h, the moisture loss became slower, especially at lower temperatures (40 °C and 45 °C).

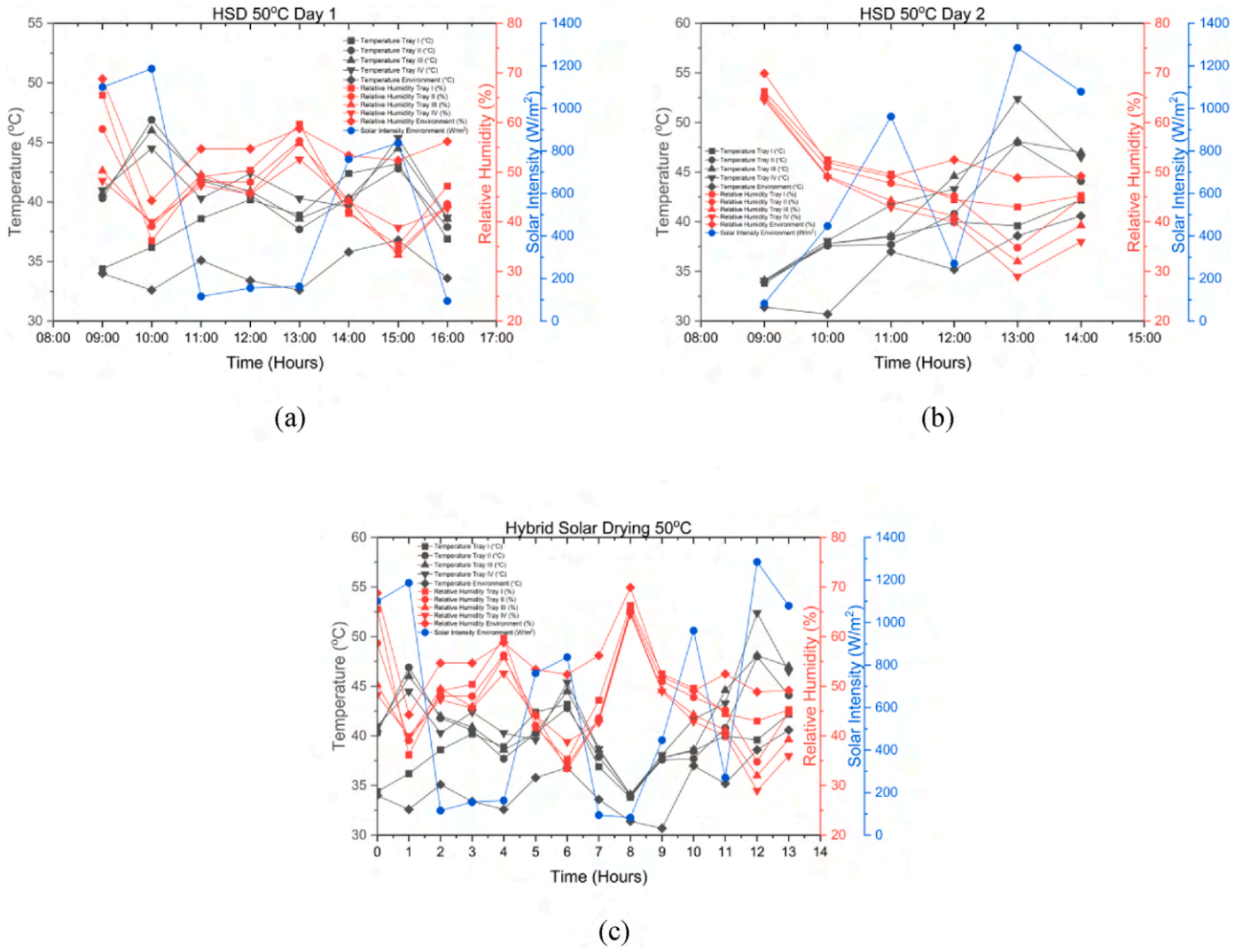

Fig. 6. Temperature profile and weather conditions on HSD 50 °C; (a) day 1; (b) day 2; and (c) overall.

The resulting 3D contours are obtained: The OSD method shows a high dependence on the ambient temperature, so its efficiency varies according to weather conditions. Higher temperatures favor better drying rates, but this method is not optimal in maintaining stability. High drying rates occur at the beginning of the process, but decrease significantly after low moisture content, mainly due to temperature fluctuations in the OSD method. HSD 40 °C Most suitable for heat-sensitive materials but takes longer to dry. The graph shows the temperature stability, which ensures that the quality of the material is maintained. HSD 45 °C provides a balance between drying speed and material protection. HSD 50 °C is very efficient for fast drying and suitable for materials that are tolerant to high temperatures. This method shows the best drying rate, ideal for materials that require a reduction in moisture in a short time. The study suggests that drying efficiency and product quality are optimally balanced at 45 °C, recommending adjustable temperature controls for diverse crop applications.

3.3. Thin layer modeling on drying kinetics

The studies reviewed demonstrate the application of different thin-layer models to assess drying behavior, with specific models proving more effective for certain materials. Higher temperatures generally increase drying rates, as seen in studies where drying rates peaked at 50 °C for cacao [55]. The relative humidity profile significantly affects drying kinetics, particularly in solar drying applications [56]. Internal diffusion was the dominant mechanism for moisture release during the drying process [57]. Semi-theoretical models provided more accurate drying behavior predictions than purely empirical ones. The study also calculated effective diffusivity and activation energy, essential parameters for scaling up drying processes [58]. Another investigation on some agricultural products highlighted using various thin-layer models, including Fick's second law-based approach. The results showed that effective moisture diffusivity values increased with temperature, confirming the relationship between temperature and moisture removal efficiency [59, 60]. Thin layer modeling of cacao bean drying is essential for optimizing processing conditions to achieve high-quality cocoa products. By employing various mathematical models and understanding the factors affecting drying kinetics [61]. Further research in this area continues to refine these models, enhancing both efficiency and product quality in cocoa processing. Tables 4–7 shows the statistical results of fitting various thin film models for OSD and HSD.

Table 4 shows that the Midili model is the best for OSD data as it provides the highest fit and the smallest prediction error, and the Logarithmic model is the second-best model after the Midili model. The Weibull model has the same R^2 and χ^2 values as the Newton model. This shows that both models have similar performance in explaining the data. However, they have the smallest fit value among all models. Table 5 shows that The Logarithmic and Midilli models again showed excellent

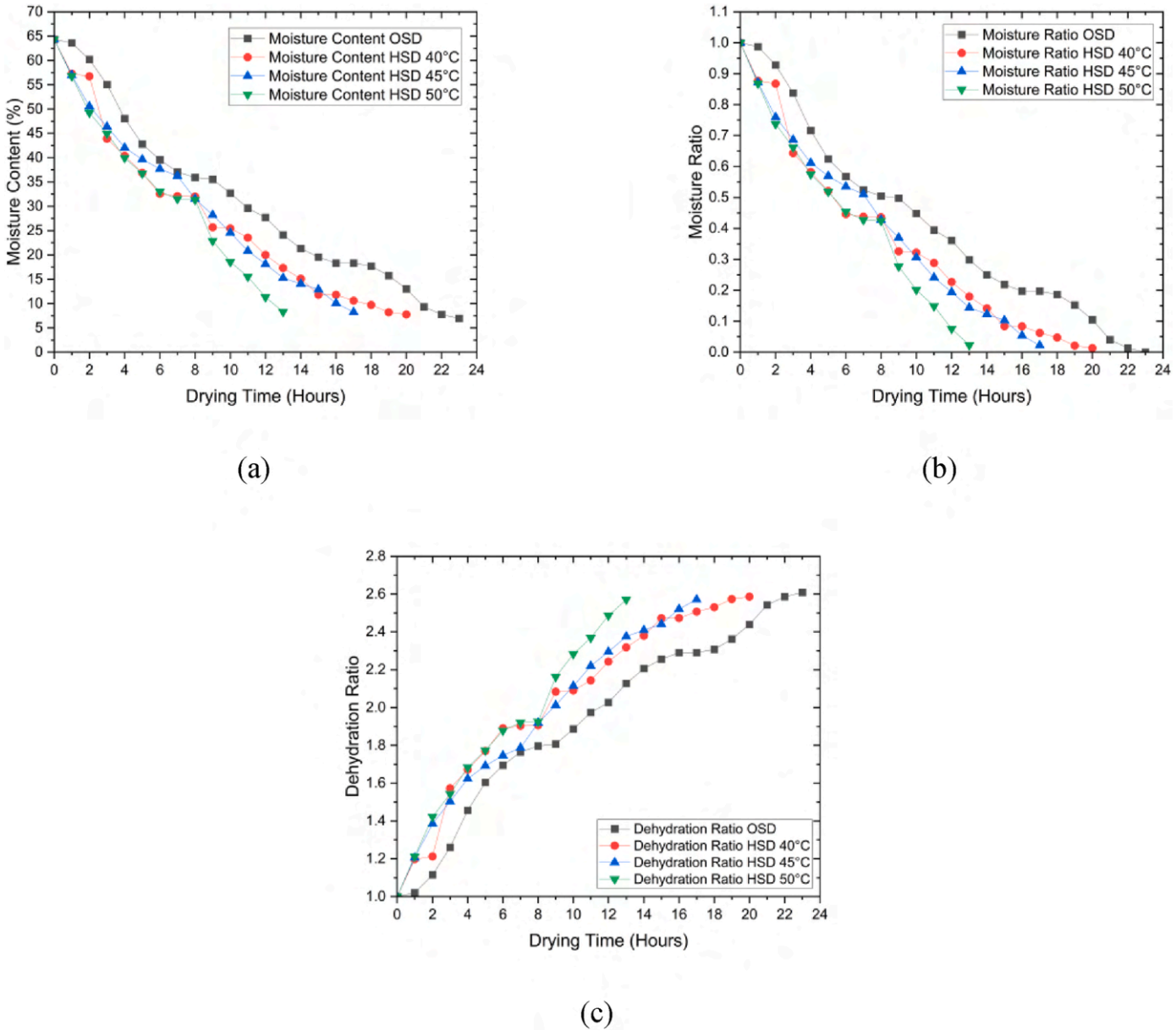

Fig. 7. Effect of changes on drying time; (a) moisture content; (b) moisture ratio; and (c) dehydration ratio.

performance with the highest R^2 and χ^2 values, and the lowest RMSE values. This indicates that these two models are suitable for predicting the drying process at 40 °C. Table 6 shows that The Logarithmic and Midilli models again showed excellent performance with the highest R^2 and χ^2 values, and the lowest RMSE values. This indicates that these two models are suitable for predicting the drying process at 45 °C. When compared to Table 5 (temperature 40 °C), in general, the models that give the best results at 45 °C tend to be similar. However, the parameter values in each model are slightly different, indicating the effect of temperature on the drying process. Table 7 shows that The Logarithmic and Midilli models again showed excellent performance with the highest R^2 and χ^2 values, and the lowest RMSE values. This indicates that both models are suitable for predicting the drying process at 50 °C. When compared with Table 5 (temperature 40 °C), Table 6 (temperature 45 °C), and the previous tables, in general, the models that gave the best results at 50 °C tended to be similar. However, the parameter values in each model were slightly different, indicating the effect of temperature on the drying process. The difference in parameter values in each model between Table 7 and the previous tables indicates that the drying temperature has a significant effect on the drying rate and the model parameters used. The Midilli model's superior performance in predicting drying kinetics ($R^2 > 0.98$) is consistent with studies on other crops such as cassava and chili, where the same model provided the best fit among several thin-layer drying model studies that uniquely contribute by integrating photovoltaic (PV) systems and LPG burners to achieve precise temperature control [62,63].

Logarithmic and Midilli models consistently showed the best performance in predicting the drying process of cocoa beans at various temperatures [64,65]. Drying temperature has a significant effect on the value of model parameters, but does not change the general trend that Logarithmic and Midilli models always give better results, in line with another research [61]. The Midilli model has a flexible structure with several adjustable parameters, so it can accommodate various forms of complex drying curves [66,67]. Likewise, the Logarithmic model has sufficient flexibility to capture changes in drying rate over time. Both models can adjust to various drying conditions, including changes in temperature, humidity, and material properties [65,68]. This allows the models to provide accurate predictions under various operating

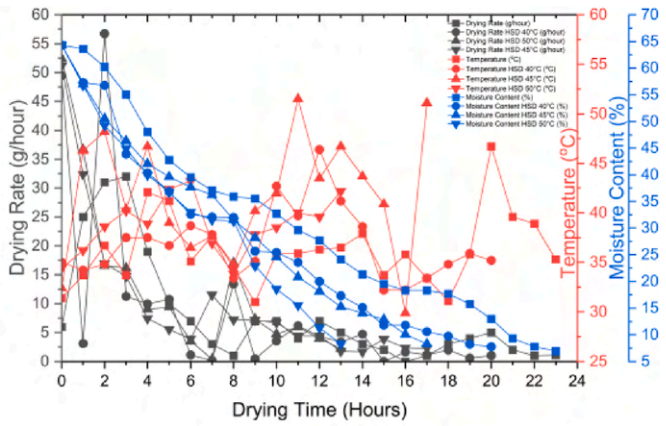

(a)

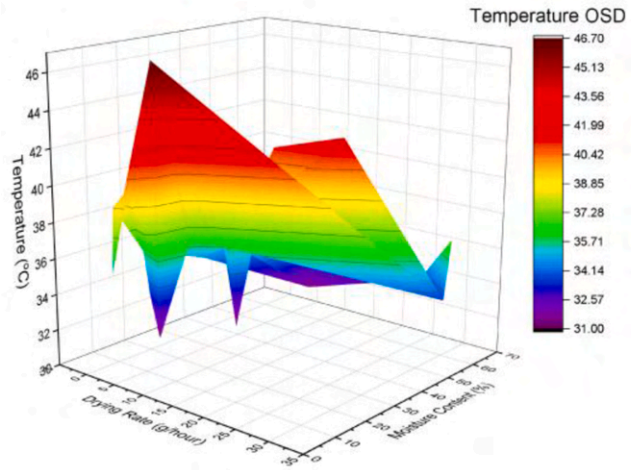

(b)

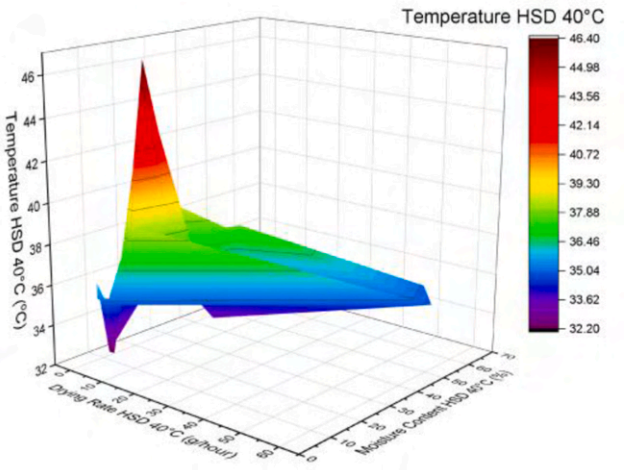

(c)

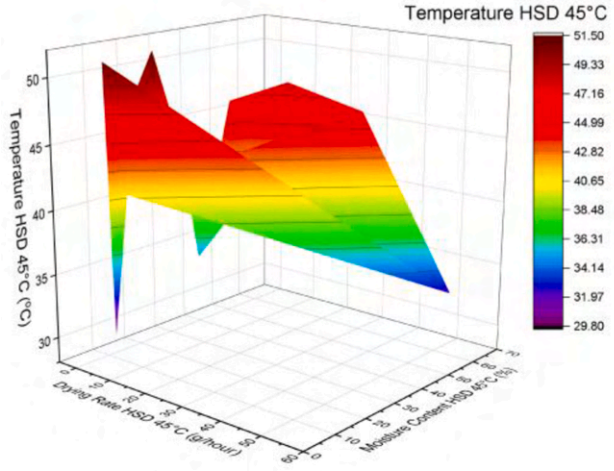

(d)

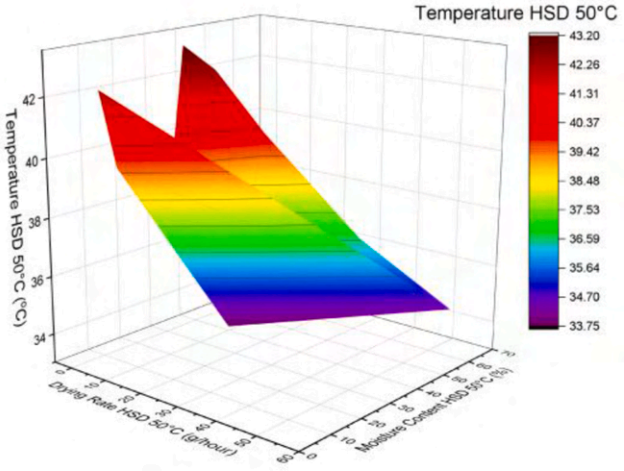

(e)

Fig. 8. Relationship between drying time and drying rate, temperature, and moisture content.; (a) 2D graphics; 3D contour from: (b) OSD; (c) HSD 40 °C; (d) HSD 45 °C, and (e) HSD 50 °C.

Table 4
Results of the fitting statistics of various thin layer models on cacao beans at OSD.

Model	Parameter	R^2	χ^2	RMSE
Newton	k = 0.0937	0.9651	0.0076	0.2751
Page	k = 0.0491, n = 1.2656	0.9830	0.0036	0.1917
Handerson-Pabis	a = 1.0844, k = 0.1021	0.9749	0.0053	0.2332
Two-term	a = 0.5422, k_1 = 0.1021, b = 0.5422, k_2 = 0.1021	0.9749	0.0053	0.2332
Logarithmic	a = 1.3295, k = 0.0611, c = -0.3003	0.9890	0.0024	0.1546
Midilli	a = 1.0390, k = 0.0797, n = 0.9556, b = -0.0083	0.9894	0.0023	0.1515
Weibull	a = 10.6769, b = 1.0000	0.9651	0.0076	0.2751
Wang & Singh	a = 0.0012, b = -0.0687	0.9866	0.0029	0.1706
Aghbashlo	k_1 = 0.0686, k_2 = -0.0205	0.9856	0.0031	0.1768

Table 5
Results of the fitting statistics of various thin layer models on cacao beans at HSD 40 °C drying temperature.

Model	Parameter	R^2	χ^2	RMSE
Newton	k = 0.1294	0.9765	0.0055	0.2052
Page	k = 0.0994, n = 1.1201	0.9807	0.0045	0.1858
Handerson-Pabis	a = 1.0279, k = 0.1331	0.9775	0.0052	0.2005
Two-term	a = 0.5139, k_1 = 0.1331, b = 0.5139, k_2 = 0.1331	0.9775	0.0052	0.2005
Logarithmic	a = 1.1501, k = 0.0939, c = -0.1637	0.9870	0.0031	0.1527
Midilli	a = 1.0108, k = 0.1311, n = 0.8799, b = -0.0081	0.9881	0.0028	0.1462
Weibull	a = 7.7292, b = 1.0000	0.9765	0.0055	0.2052
Wang & Singh	a = 0.0024, b = -0.0957	0.9804	0.0045	0.1870
Aghbashlo	k_1 = 0.1071, k_2 = -0.0166	0.9840	0.0037	0.1692

Table 6
Results of the fitting statistics of various thin layer models on cacao beans at HSD 45 °C drying temperature.

Model	Parameter	R^2	χ^2	RMSE
Newton	k = 0.1248	0.9691	0.0059	0.2128
Page	k = 0.0856, n = 1.1740	0.9770	0.0044	0.1833
Handerson-Pabis	a = 1.0187, k = 0.1273	0.9696	0.0058	0.2107
Two-term	a = 0.5094, k_1 = 0.1273, b = 0.5094, k_2 = 0.1273	0.9696	0.0058	0.2107
Logarithmic	a = 1.4891, k = 0.0581, c = -0.5319	0.9928	0.0014	0.1024
Midilli	a = 1.0000, k = 0.1209, n = 0.6478, b = -0.0272	0.9953	0.0009	0.0830
Weibull	a = 8.0146, b = 1.0000	0.9691	0.0059	0.2128
Wang & Singh	a = 0.0021, b = -0.0918	0.9878	0.0023	0.1333
Aghbashlo	k_1 = 0.0931, k_2 = -0.0259	0.9865	0.0026	0.1404

conditions. Although the form of the mathematical equations is different, both models have a reasonable physical basis for describing the drying process. They consider factors such as evaporation rate, diffusion of water vapor in the material, and resistance to mass transfer. It is important to remember that the mathematical model is only a simplified representation of a complex phenomenon and other factors not included in the model can affect the actual drying results. In line with the findings, the logarithmic model provides good results under all conditions including for the air flow rate variable [69].

Table 7
Results of the fitting statistics of various thin layer models on cacao beans at HSD 50 °C drying temperature.

Model	Parameter	R^2	χ^2	RMSE
Newton	k = 0.1448	0.9556	0.0078	0.2240
Page	k = 0.1023, n = 1.1773	0.9638	0.0063	0.2023
Handerson-Pabis	a = 1.0213, k = 0.1483	0.9565	0.0076	0.2218
Two-term	a = 0.5106, k_1 = 0.1483, b = 0.5106, k_2 = 0.1483	0.9565	0.0076	0.2218
Logarithmic	a = 2.0403, k = 0.0455, c = -1.0872	0.9847	0.0027	0.1315
Midilli	a = 1.0020, k = 0.1170, n = 0.3888, b = -0.0538	0.9903	0.0017	0.1045
Weibull	a = 6.9051, b = 1.0000	0.9556	0.0078	0.2240
Wang & Singh	a = 0.0024, b = -0.1038	0.9789	0.0037	0.1546
Aghbashlo	k_1 = 0.1053, k_2 = -0.0341	0.9747	0.0044	0.1691

3.4. Energy and exergy analysis of dried cacao beans on the open sun drying and photovoltaic and LPG burner assisted hybrid solar drying system

Table 8 shows a data table comparing various energy and sustainability parameters of several drying processes. Energy Utilization (EU) is the amount of energy used in kilojoules per second. The OSD method has deficient energy consumption (0.0008 kJ/s) and HSD at temperatures of 40 °C, 45 °C, and 50 °C shows much higher energy consumption. The energy utilization ratio (EUR) shows relative efficiency. The value is very small for OSD (0.0008) and larger for HSD, increasing with temperature. For hybrid solar-hot air drying, EURs between 0.056 and 0.957 were found, demonstrating the potential for high efficiency under optimal conditions [70]. Exergy loss (EX_L) or loss of "exergy" during the process. OSD shows the highest exergy loss (0.0562 kJ/s). EX_L in HSD decreases at higher temperatures, with the lowest value at HSD 45 °C (0.0062 kJ/s). Exergy Efficiency (EX_{Eff}) is how efficiently energy is utilized in the process. OSD has the lowest efficiency (65.165 %). HSD 45 °C shows the highest efficiency (94.661 %). Improvement potential rate (IP) or potential improvement in energy efficiency. The greatest IP is in OSD (0.0179 kJ/s). HSD shows lower IP, decreasing with increasing efficiency. The potential rate of improvement is significant when solar-biomass hybrid technologies are integrated. These systems can utilize residual heat, reducing operating costs and increasing drying efficiency [71]. A higher sustainability index (SI) indicates a more sustainable process. OSD has the lowest index (3.1412), while HSD 45 °C has the highest index (18.731). HSD 45 °C is the most energy-efficient and sustainable method, with low exergy loss, high efficiency, and the highest SI. OSD has the lowest efficiency and sustainability, although the energy used is very small. Increasing the temperature in HSD reduces the potential for improvement but increases efficiency and sustainability up to the optimum point (45 °C). Sustainability metrics for cocoa drying processes can be improved by using renewable energy sources and efficient drying technologies. Using solar energy in conjunction with biomass can reduce carbon footprints and improve sustainability metrics [71,72].

The drying efficiency and energy utilization findings from this study align with existing research that emphasizes the advantages of hybrid solar drying systems over traditional open sun drying (OSD). The reduction in drying time from 23 hours (OSD) to as low as 13 hours (HSD at 50 °C) corresponds with findings from Adejumo et al., where hybrid solar dryers significantly decreased drying times for agricultural products compared to conventional methods [6]. High exergy efficiency (up to 94.66 %) and a sustainability index of 18.73 for HSD at 45 °C. This surpasses the energy metrics reported in prior research on solar drying systems, where exergy efficiencies typically ranged between 22.77 % and 27.90 % [73]. Furthermore, the content of 7–8% in cocoa beans outperforms traditional OSD's moisture variability, which often remains above 17 %, aligning with quality parameters critical for cocoa

Table 8
Energy-exergy analysis of dried cacao beans on OSD and HSD.

Dying type	Energy utilization (kJ/s)	Energy utilization ratio (−)	Exergy loss (kJ/s)	Exergy efficiency (%)	Improvement potential rate (kJ/s)	Sustainability index (−)
OSD	0.0008	0.0008	0.0562	65.1654	0.0179	3.1412
HSD 40 °C	42.6570	0.3001	0.0184	85.8973	0.0026	7.0909
HSD 45 °C	47.9721	0.3246	0.0062	94.6614	0.0003	18.7314
HSD 50 °C	35.6288	0.2772	0.0210	86.3601	0.0029	7.3314

processing [74,75].

In contrast to studies focusing on simpler hybrid systems, such as biogas-assisted dryers, this study's incorporation of PV systems addresses energy challenges during low sunlight conditions, ensuring uninterrupted drying cycles. This advancement not only enhances the applicability of hybrid systems in diverse climatic zones but also offers a scalable solution for smallholder farmers aiming to modernize their post-harvest processing practices. The incorporation of PV systems ensures that drying processes can continue even during periods of low solar radiation, thereby providing a more reliable energy source compared to simpler hybrid systems like biogas-assisted dryers. This is crucial for maintaining uninterrupted drying cycles, which is essential for preserving product quality and reducing post-harvest losses [76,77].

Despite these advancements, challenges persist in the regulatory and technical expertise required for implementing HSD systems. Previous studies have suggested that integrating additional renewable energy sources and optimizing component design could mitigate these barriers, a recommendation this study reinforces for future research.

4. Conclusion

This study comprehensively compares the performance of open sun drying (OSD) and photovoltaic and LPG burner assisted hybrid solar drying system (HSD) systems for cocoa beans. OSD, though widely used for its simplicity and low cost, demonstrated significant limitations, including prolonged drying durations of up to 3.5 days, inconsistent moisture reduction to around 17.4 %, and susceptibility to environmental contamination. In contrast, HSD systems effectively reduced drying time and achieved target moisture content levels of 7–8% within controlled conditions. The experimental findings revealed that HSD could achieve a thermal efficiency of up to 72.36 % and an exergy efficiency ranging from 22.77 % to 27.90 %, significantly surpassing the performance metrics of OSD. The drying kinetics analysis confirmed that the Midili model, with an $R^2 > 0.98$, provided the most accurate representation of moisture removal at drying temperatures of 40 °C, 45 °C, and 50 °C. For example, HSD systems reduced moisture from 65 % to below 8 % within 13–20 hours, a remarkable improvement compared to the 23 hours needed for similar results in OSD. HSD also demonstrated energy efficiency with specific energy consumption as low as 2.75 kWh/kg and significant environmental benefits, including reducing CO_2 emissions by up to 60.29 tons. These findings underscore the system's capability to preserve product quality while improving operational efficiency and sustainability. However, barriers to the widespread adoption of HSD include higher initial costs and technical expertise requirements. Future research should focus on cost-effective designs, enhancing scalability, and integrating additional renewable energy sources to address these challenges. Overall, HSD offers a promising pathway to more efficient, high-quality, and sustainable drying processes in agricultural production.

While this study advances the understanding of hybrid solar drying technologies, several areas warrant further investigation to enhance their applicability and efficiency, such as: Cost optimization to investigate innovative designs and materials to reduce the initial investment costs associated with HSD systems, making them more accessible to smallholder farmers. The integration of advanced renewable energy technologies to explore the use of advanced photovoltaic systems, such as bifacial panels or perovskite solar cells, to further improve energy efficiency and performance under variable climatic conditions. Automation and control systems to develop smart sensors and automated control systems to optimize drying parameters, reducing the need for constant human intervention. Scalability studies assess the scalability of HSD systems for large-scale agricultural operations and evaluate their performance across diverse crops and environmental conditions. Energy storage solutions to investigate the integration of energy storage systems, such as thermal batteries, to ensure consistent drying performance during low sunlight periods. Environmental impact assessment to conduct a detailed life cycle assessment (LCA) to quantify the long-term environmental benefits of adopting HSD technologies and compare them with other renewable drying methods. Economic feasibility studies to perform comprehensive cost-benefit analyses in different agricultural settings to validate the economic advantages of HSD systems. By addressing these areas, future studies can build on the findings of this research, paving the way for more efficient, sustainable, and widely adopted drying technologies in agricultural production.

CRediT authorship contribution statement

Tubagus Rayyan Fitra Sinuhaji: Writing – review & editing, Writing – original draft, Visualization, Project administration, Methodology, Funding acquisition, Conceptualization. **Suherman Suherman:** Writing – review & editing, Writing – original draft, Validation, Supervision, Conceptualization. **Hadiyanto Hadiyanto:** Writing – review & editing, Writing – original draft, Validation, Supervision, Conceptualization. **Ardi Ardan:** Writing – review & editing, Writing – original draft, Investigation, Conceptualization. **Sulistia Rahmawati:** Writing – review & editing, Writing – original draft, Investigation, Conceptualization.

Funding

This research is financially supported by the Direktorat Riset Teknologi, dan Pengabdian Masyarakat, Direktorat Jenderal Pendidikan Tinggi, Riset, dan Teknologi, Kementerian Pendidikan, Kebudayaan Riset dan Teknologi Republik Indonesia (Ministry of Education, Culture, Research, and Technology/KEMDIKBUDRISTEK), through the PMDSU Research Grant to Diponegoro University with No: 601-87/UN7.D2/PP/VI/2024.

Declaration of competing interest

The authors declare the following financial interests/personal relationships which may be considered as potential competing interests: Tubagus Rayyan Fitra Sinuhaji reports financial support was provided by Ministry of Education Culture Research and Technology. Tubagus Rayyan Fitra Sinuhaji reports a relationship with Ministry of Education Culture Research and Technology that includes: funding grants. If there are other authors, they declare that they have no known competing financial interests or personal relationships that could have appeared to influence the work reported in this paper.

Acknowledgments

The author would like to express his deepest appreciation to all laboratory staff at the Waste Treatment Laboratory, Department of Chemical Engineering, Faculty of Engineering, Diponegoro University for their assistance and use of the laboratory for the research process. For their role in making this research a success.

Data availability

No data was used for the research described in the article.

References

[1] I. López Cerino, E. Chávez García, Eficacia de secador solar tipo túnel con cacao (Theobroma Cacao L.) en Tabasco, Rev Mex De Cienc Agric (2018) 4395–4405, https://doi.org/10.29312/remexca.v0i21.1528.
[2] C.A. Komolafe, M.A. Waheed, S.I. Kuye, B.A. Adewumi, I.O. Oluwaleye, T.M. A. Olayanju, Sun drying of cocoa with firebrick thermal storage materials, Int. J. Energy Res. 44 (2020), https://doi.org/10.1002/er.5364.
[3] B.F. Dzelagha, N.M. Ngwa, D.N. Bup, A review of cocoa drying technologies and the effect on bean quality parameters, Int J Food Sci 2020 (2020), https://doi.org/10.1155/2020/8830127.
[4] J.H. de O. Sales, L.V. de M. Soglia, P.H.S. Girotto, C.S. de S. Brandão, Drying system via solar energy and heat accumulator for almond's cocoa, CONTRIBUCIONES A LAS CIENCIAS SOCIALES 16 (2023), https://doi.org/10.55905/revconv.16n.10-119.
[5] N. Kalita, P. Muthukumar, A. Dalal, Performance investigation of a hybrid solar dryer with electric and biogas backup air heaters for chilli drying, Therm. Sci. Eng. Prog. 52 (2024) 102646, https://doi.org/10.1016/j.tsep.2024.102646.
[6] P.O. Adejumo, J.A.V. Olumurewa, M.K. Bolade, O.O. Awolu, Development and performance evaluation of hybrid-solar dryer for cassava grate, Asian Food Science Journal 22 (2023), https://doi.org/10.9734/afsj/2023/v22i10671.
[7] Y. Martin, F. Henriquez, O. Melgar, L. Mogollon, Evaluation of a cocoa solar dryer prototype in cilico creek, ngabe bugle, in: Proceedings - 2022 8th International Engineering, Sciences and Technology Conference, 2022, https://doi.org/10.1109/IESTEC54539.2022.00081. IESTEC 2022.
[8] R. Khathir, E. Kurniawan, Y. Yunita, S. Syafriandi, Drying characteristics of cacao beans using modified solar tunnel dryer type hohenheim, Aceh Int. J. Sci. Technol. 12 (2023), https://doi.org/10.13170/aijst.12.3.30246.
[9] T.O. Aduewa, S.A. Fatounde, A.M. Aderotoye, A comprehensive review of the hybrid solar dryers, Asian Journal of Advances in Agricultural Research (2022), https://doi.org/10.9734/ajaar/2022/v18i330224.
[10] J.K. Andharia, B. Markam, J. Patel, S. Maiti, Study of a mixed-mode solar dryer integrated with photovoltaic powered dehumidifier, Sol. Energy 273 (2024) 112505, https://doi.org/10.1016/j.solener.2024.112505.
[11] A.P. Singh, A. Gupta, A. Biswas, B. Das, Experimental study of a novel photovoltaic-thermal-thermoelectric generator-based solar dryer for grapes drying, Int. J. Green Energy 21 (2024), https://doi.org/10.1080/15435075.2023.2244046.
[12] B. Aktekelī, M. Aktaş, M. Koşan, E. Arslan, Experimental examination of solar-powered compact dryer integrated with the new photovoltaic thermal heat pump hybrid system. https://doi.org/10.2139/ssrn.4817036, 2024.
[13] S. Suherman, H. Hadiyanto, N. Franz, V. Kamandjaja, T.R.F. Sinuhaji, Energy analysis and economy performance of a hybrid solar dryer for drying coffee, Jurnal Sains Materi Indonesia 26 (2024) 25–34, https://doi.org/10.55981/jsmi.2024.3135.
[14] A.M. Antunes, F.L. Gaia, J.W.L. Rodrigues, M.K. da C. de Araujo, C.F. Lisboa, A. B. Pacheco, B.S. Fjiyama, E.T. de Andrade, Mathematical modeling of drying kinetics of two varieties of cacao cultivated in the brazilian amazon region, CONTRIBUCIONES A LAS CIENCIAS SOCIALES 17 (2024) e8697, https://doi.org/10.55905/revconv.17n.7-338.
[15] S. Suherman, H. Widuri, S. Patricia, E.E. Susanto, R.J. Sutrisna, Energy analysis of a hybrid solar dryer for drying coffee beans, Int. J. Renew. Energy Dev. 9 (2020), https://doi.org/10.14710/ijred.9.1.131-139.
[16] A. Afzal, T. Iqbal, K. Ikram, M.N. Anjum, M. Umair, M. Azam, S. Akram, F. Hussain, M. Ameen ul Zaman, A. Ali, F. Majeed, Development of a hybrid mixed-mode solar dryer for product drying, Heliyon 9 (2023) e14144, https://doi.org/10.1016/j.heliyon.2023.e14144.
[17] S.F. Dina, H. Ambarita, F.H. Napitupulu, H. Kawai, Study on effectiveness of continuous solar dryer integrated with desiccant thermal storage for drying cocoa beans, Case Stud. Therm. Eng. 5 (2015), https://doi.org/10.1016/j.csite.2014.11.003.
[18] B.F. Suherman, H. Satriadi, O. Yuariski, R.S. Nugroho, A. Shobib, Thin layer drying kinetics of of roselle, Adv. J. Food Sci. Technol. 4 (2012).
[19] S. Suherman, H. Hadiyanto, M.A. Asy-Syaqiq, G. 'Afifah Ghassani, M. Ajundasari, Energy and exergy performance evaluation of a drying coffee beans system using a photovoltaic–direct solar dryer at different drying temperature conditions, Int. J. Ambient Energy 45 (2024), https://doi.org/10.1080/01430750.2024.2344548.
[20] B.K. Koua, P.M.E. Koffi, P. Gbaha, Evolution of shrinkage, real density, porosity, heat and mass transfer coefficients during indirect solar drying of cocoa beans, Journal of the Saudi Society of Agricultural Sciences 18 (2019), https://doi.org/10.1016/j.jssas.2017.01.002.
[21] M. da S. do Nascimento, P.O. Pena, D.M. Brum, F.T. Imazaki, M.L.S.A. Tucci, P. Efraim, Behavior of Salmonella during fermentation, drying and storage of cocoa beans, Int. J. Food Microbiol. 167 (2013), https://doi.org/10.1016/j.ijfoodmicro.2013.10.003.
[22] V.L. Deus, M.B. de Cerqueira E Silva, L.F. Maciel, L.C.R. Miranda, E.Y. Hirooka, S. E. Soares, E. de Souza Ferreira, E. da Silva Bispo, Influence of drying methods on cocoa (Theobroma cacao L.): antioxidant activity and presence of ochratoxin A, Food Sci. Technol. 38 (2018), https://doi.org/10.1590/fst.09917.
[23] E. Romanens, R. Näf, T. Lobmaier, V. Pedan, S.F. Leischtfeld, L. Meile, S. M. Schwenninger, A lab-scale model system for cocoa bean fermentation, Appl. Microbiol. Biotechnol. 102 (2018), https://doi.org/10.1007/s00253-018-8835-6.
[24] S. Suherman, M. Djaeni, D.H. Wardhani, M.R. Dzaki, M.N.F. Bagas, Performance analysis of solar tray dryer for cassava starch, in: MATEC Web of Conferences, 2018, https://doi.org/10.1051/matecconf/201815605008.
[25] J. Puello-Mendez, P. Meza-Castellar, L. Cortés, L. Bossa, E. Sanjuan, H. Lambis-Miranda, L. Villamizar, Comparative study of solar drying of cocoa beans: two methods used in Colombian rural areas, Chem Eng Trans 57 (2017), https://doi.org/10.3303/CET1757286.
[26] O. Bin Hameed, H. Ahsan, A.H. Rather, S.Z. Hussain, H.R. Naik, Influence of pretreatments and drying methods on water activity, dehydration and rehydration ratio of dried tomato, Biosci Biotechnol Res Asia 13 (2016), https://doi.org/10.13005/bbra/2391.
[27] Z. Parhizi, H. Karami, I. Golpour, M. Kaveh, M. Szymanek, A.M. Blanco-Marigorta, J.D. Marcos, E. Khalife, S. Skowron, N. Adnan Othman, Y. Darvishi, Modeling and optimization of energy and exergy parameters of a hybrid-solar dryer for basil leaf drying using RSM, Sustainability 14 (2022), https://doi.org/10.3390/su14148839.
[28] C.L. Hii, C.L. Law, M. Cloke, Modeling using a new thin layer drying model and product quality of cocoa, J. Food Eng. 90 (2009), https://doi.org/10.1016/j.jfoodeng.2008.06.022.
[29] A. Dasore, R. Konijeti, N. Puppala, Method for determining the appropriate thin layer drying model for a feedstock, Int. J. Recent Technol. Eng. 8 (2019), https://doi.org/10.35940/ijrte.C5335.098319.
[30] N.A. Latiff, L.C. Abdullah, P.Y. Ong, N.A.M. Amin, Thin-layer drying model of cosmos caudatus, Chem. Ind. Chem. Eng. Q. 27 (2021), https://doi.org/10.2298/CICEQ191121038L.
[31] A.S. Kipcak, I. Doymaz, Mathematical modeling and drying characteristics investigation of black mulberry dried by microwave method, Int. J. Fruit Sci. 20 (2020), https://doi.org/10.1080/15538362.2020.1782805.
[32] L.A. Duc, N. Hay, P. Van Kien, Mathematical model of thin layer drying of ganoderma lucidum by radio frequency assisted heat pump drying, Frontiers in Heat and Mass Transfer 18 (2022), https://doi.org/10.5098/hmt.18.44.
[33] O. Corzo, N. Bracho, C. Alvarez, Weibull model for thin-layer drying of mango slices at different maturity stages, J. Food Process. Preserv. 34 (2010), https://doi.org/10.1111/j.1745-4549.2009.00433.x.
[34] B.M.A. Amer, M.M. Azam, A.G. Saad, Monitoring temperature profile and drying kinetics of thin-layer banana slices under controlled forced convection conditions, Processes 11 (2023), https://doi.org/10.3390/pr11061771.
[35] A.M. Sefidan, M. Sellier, J.N. Hewett, A. Abdollahi, G.R. Willmott, S.M. Becker, Wet-core temperature and concentration profiles in a single skim milk droplet drying process, Appl. Therm. Eng. 212 (2022), https://doi.org/10.1016/j.applthermaleng.2022.118571.
[36] D. Qiu, R. Duan, Y. Wang, Y. He, C. Li, X. Shen, Y. Li, Effects of different drying temperatures on the profile and sources of flavor in semi-dried golden pompano (Trachinotus ovatus), Food Chem. 401 (2023), https://doi.org/10.1016/j.foodchem.2022.134112.
[37] M.W. Kareem, K. Habib, S.A. Sulaiman, Numerical and experimental investigation of direct solar crop dryer for farmers, in: AIP Conf Proc, 2015, https://doi.org/10.1063/1.4919209.
[38] M.S. Sodha, P.K. Bansal, A. Dang, S.B. Sharma, Open sun drying: an analytical study, Dry. Technol. 3 (1985), https://doi.org/10.1080/07373938508916295.
[39] A. Castañeda-Miranda, R. Castañeda-Miranda, J. Meza Jimenez, Solar drying system for the agro-products dehydration, J. Agric. Soc. Sci. 4 (2008).
[40] P. Meas, A.H.J. Paterson, D.J. Cleland, J.E. Bronlund, J. Mawson, A. Hardacre, J. F. Rickman, Relating rice grain quality to conditions during sun drying, Int. J. Food Eng. 9 (2013), https://doi.org/10.1515/ijfe-2013-0019.
[41] S. Suherman, N.P. Barokah, N.A. Islamiaty, H. Hadiyanto, T.R.F. Sinuhaji, B.W.H. E. Prasetiyono, A. Lomi, R.H. Setyobudi, M.I. Massadeh, E. Yandri, Assessment on hybrid solar dryer for an effective red chili drying process, in: E3S Web of Conferences, 2023, https://doi.org/10.1051/e3sconf/202343200035.
[42] A. Fudholi, M.Y. Othman, M.H. Ruslan, M. Yahya, A. Zaharim, K. Sopian, The effects of drying air temperature and Humidity on the drying kinetics of seaweed, in: Recent Researches in Geography, Geology, Energy, Environment and Biomedicine - Proc. Of the 4th WSEAS Int. Conf. on EMESEG'11, 2nd Int. Conf. on WORLD-GEO'11, 5th Int. Conf. on EDEB'11, 2011.
[43] A.S.M. Hii CL, S.V. Jangam, S.P. Ong, Solar Drying: Fundamentals,Applications and Innovations, 2012.
[44] A.R. Caparanga, R.A.L. Reyes, R.L. Rivas, F.C. De Vera, V. Retnasamy, H. Aris, Effects of air temperature and velocity on the drying kinetics and product particle size of starch from arrowroot (Maranta arundinacae), in: EPJ Web Conf, 2017, https://doi.org/10.1051/epjconf/201716201084.
[45] P.R. Nabila, R. Ratnawati, M. Djaeni, Moisture removal observation of onion slice drying at various temperature, in: AIP Conf Proc, 2023, https://doi.org/10.1063/5.0112555.

[46] L.L. Macedo, W.C. Vimercati, C. da Silva Araújo, S.H. Saraiva, L.J.Q. Teixeira, Effect of drying air temperature on drying kinetics and physicochemical characteristics of dried banana, J. Food Process. Eng. 43 (2020), https://doi.org/10.1111/jfpe.13451.
[47] D.I. Onwude, N. Hashim, R.B. Janius, N. Nawi, K. Abdan, Modelling effective moisture diffusivity of pumpkin (Cucurbita moschata) slices under convective hot air drying condition, Int. J. Food Eng. 12 (2016), https://doi.org/10.1515/ijfe-2015-0382.
[48] N. Tashiev, Investigation of the temperature dependence of a product dried in a solar dryer on its moisture content, Bulletin of Science and Practice 9 (2023), https://doi.org/10.33619/2414-2948/89/42.
[49] C.E. Henry, T.N. Jospeh, E.O. Chijioke, O.N. Charles, Optimum process parameters and thermal properties of moisture content reduction in water yam drying, Asian Journal of Chemical Sciences (2021), https://doi.org/10.9734/ajocs/2021/v9i419080.
[50] O.I. Obajemihi, J.O. Olaoye, J.H. Cheng, J.O. Ojediran, D.W. Sun, Optimization of process conditions for moisture ratio and effective moisture diffusivity of tomato during convective hot-air drying using response surface methodology, J. Food Process. Preserv. 45 (2021), https://doi.org/10.1111/jfpp.15287.
[51] I.S. Čubrić, G. Čubrić, V.M.P. Matković, Fluid transfer properties of functional materials, in: 2023 7th International Conference on Automation, Control and Robots, ICACR 2023, 2023, https://doi.org/10.1109/ICACR59381.2023.10314643.
[52] X. Huang, T. Qi, Z. Wang, D. Yang, X. Liu, A moisture transmembrane transfer model for pore network simulation of plant materials drying, Dry. Technol. 30 (2012), https://doi.org/10.1080/07373937.2012.718306.
[53] B. Xiao, J. Chang, X. Huang, X. Liu, A moisture transfer model for isothermal drying of plant cellular materials based on the pore network approach, Dry. Technol. 32 (2014), https://doi.org/10.1080/07373937.2014.883629.
[54] X. Song, J. Wei, Z. Mao, X. Chi, Z. Zhu, G. Han, W. Cheng, Effect of hot-air drying conditions on the drying efficiency and performance of a waterborne coating on pine wood, Forests 14 (2023), https://doi.org/10.3390/f14091752.
[55] A.A. Obisanya, G.O. Ajiboye, I.O. Ajiboshin, O.I. Ogunyemi, Drying kinetics and thin layer modelling of clerodendrum volubile (marugbo) leaves, International Journal of Chemical Engineering and Applications 13 (2022), https://doi.org/10.18178/ijcea.2022.13.4.796.
[56] A. Alami, L. Rajaoarisoa, M.H. Benzaama, A. Benbakhti, Drying model based on the relative humidity profile of thin-layer tomatoes in an indirect solar dryer, J. Therm. Eng. 9 (2023), https://doi.org/10.18186/THERMAL.1401040.
[57] C.T. Ee, Y.J. Khaw, C.L. Hii, C.L. Chiang, M. Djaeni, Drying kinetics and modelling of convective drying of kedondong fruit, ASEAN Journal of Chemical Engineering 21 (2021), https://doi.org/10.22146/ajche.62932.
[58] O.Y. Turan, F.E. Firatligil, Modelling and characteristics of thin layer convective air-drying of thyme (Thymus vulgaris) leaves, Czech J. Food Sci. 37 (2019), https://doi.org/10.17221/243/2017-CJFS.
[59] M. Popescu, P. Iancu, V. Plesu, C.S. Bildea, F.A. Manolache, Mathematical modeling of thin-layer drying kinetics of tomato peels: influence of drying temperature on the energy requirements and extracts quality, Foods 12 (2023), https://doi.org/10.3390/foods12203883.
[60] A.S. Oyerinde, Modelling of thin layer drying kinetics of tomato (Lycopersicon esculentum mill) slices under direct sun and air assisted solar dryer, International Journal of Engineering and Applied Sciences IJEAS 3 (2016).
[61] H. Moussaoui, A. Idlimam, A. Lamharrar, The characterization and modeling kinetics for drying of taraxacum officinale leaves in a thin layer with a convective solar dryer, in: Lecture Notes in Electrical Engineering, 2019, https://doi.org/10.1007/978-981-13-1405-6_75.
[62] B.D. Argo, S. Sandra, U. Ubaidillah, Mathematical modeling on the thin layer drying kinetics of cassava chips in a multipurpose convective-type tray dryer heated by a gas burner, J. Mech. Sci. Technol. 32 (2018), https://doi.org/10.1007/s12206-018-0646-2.
[63] S.D.F. Mihindukulasuriya, H.P.W. Jayasuriya, Mathematical modeling of drying characteristics of chilli in hot air oven and fluidized bed dryers, Agricultural Engineering International: CIGR Journal 15 (2013).
[64] S.M. Say, T. Erdem, K. Ekinci, B.O. Erdem, M. Sehri, S.K. Sumer, Drying kinetics of olive pomace-derived charcoal briquettes with energy consumption, Semina Ciências Agrárias 43 (2022), https://doi.org/10.5433/1679-0359.2022V43N4P1805.
[65] D.S.C. Soares, D.G. Costa, A.K.S. Abud, T.P. Nunes, A.M. Oliveira Júnior, The use of performance indicators for evaluating models of drying jackfruit (artocarpus heterophyllus, international journal of biological, biomolecular, agricultural, Food and Biotechnological Engineering 8 (2014).
[66] R. Ishaq, S. Bekhor, Y. Shiftan, Flexible model structure for discrete-choice models. Proceedings of the Institution of Civil Engineers: Transport 165, 2012, https://doi.org/10.1680/tran.10.00001.
[67] R. Ishaq, S. Bekhor, Y. Shiftan, A flexible model structure approach for discrete choice models, Transportation 40 (2013), https://doi.org/10.1007/s11116-012-9431-8.
[68] V.T. Nguyen, M.D. Le, Influence of various drying conditions on phytochemical compounds and antioxidant activity of carrot peel, Beverages 4 (2018), https://doi.org/10.3390/beverages4040080.
[69] H. Moussaoui, K. Chatir, A.D. Tuncer, A. Khanlari, M. Kouhila, A. Idlimam, A. Lamharrar, Improving environmental sustainability of food waste using a solar dryer: analyzing drying kinetics and biogas production potential, Sol. Energy 269 (2024), https://doi.org/10.1016/j.solener.2024.112341.
[70] M. Kaveh, H. Karami, A. Jahanbakhshi, Investigation of mass transfer, thermodynamics, and greenhouse gases properties in pennyroyal drying, J. Food Process. Eng. 43 (2020), https://doi.org/10.1111/jfpe.13446.
[71] A.D. Rincón-Quintero, L.A. Del Portillo-Valdés, A. Meneses-Jácome, C.L. Sandoval-Rodríguez, W.L. Rondón-Romero, J.G. Ascanio-Villabona, Trends in technological advances in food dehydration, identifying the potential extrapolated to cocoa drying: a bibliometric study, in: Lecture Notes in Electrical Engineering, 2021, https://doi.org/10.1007/978-3-030-72212-8_13.
[72] A. Piri, A. Hazervazifeh, Thermodynamic performance of hot air drying system: energy and exergy analysis for wet glass containers in honey processing plant, J. Food Process. Eng. 47 (2024), https://doi.org/10.1111/jfpe.14741.
[73] P. Sudhakar, A review on performance enhancement of solar drying systems, IOP Conf. Ser. Mater. Sci. Eng. 1130 (2021), https://doi.org/10.1088/1757-899x/1130/1/012042.
[74] A. Ibrahim, I. Elsebaee, A. Amer, G. Aboelasaad, A. El-Bediwy, M. El-Kholy, Development and evaluation of a hybrid smart solar dryer, J. Food Sci. 88 (2023), https://doi.org/10.1111/1750-3841.16713.
[75] S. Prem Kumar, G. Kumar, Evaluation of energy performances of solar dryers, Iranian Journal of Energy and Environment 14 (2023), https://doi.org/10.5829/ijee.2023.14.01.08.
[76] E.-S.G. Khater, A.H. Bahnasawy, A.A.T. Oraiath, S.K. Alhag, L.A. Al-Shuraym, M. E. Moustapha, A.E. Elwakeel, A. Elbeltagi, A. Salem, K.A. Metwally, M.A.I. Abdalla, M.M. Hussein, M.A. Abdeen, Assessment of a LPG hybrid solar dryer assisted with smart air circulation system for drying basil leaves, Sci. Rep. 14 (2024) 23922, https://doi.org/10.1038/s41598-024-74751-4.
[77] S. Gorjian, B. Hosseingholilou, L.D. Jathar, H. Samadi, S. Samanta, A.A. Sagade, K. Kant, R. Sathyamurthy, Recent advancements in technical design and thermal performance enhancement of solar greenhouse dryers, Sustainability 13 (2021), https://doi.org/10.3390/su13137025.